United Nations Scientific Committee on the Effects of Atomic Radiation

ATTACHMENT A-9

ATMOSPHERIC TRANSPORT, DISPERSION AND DEPOSITION MODELLING OF AIR CONCENTRATION OVER JAPAN

UNSCEAR 2020/2021 Report, Annex B, Levels and effects of radiation exposure due to the accident at the Fukushima Daiichi Nuclear Power Station: implications of information published since the UNSCEAR 2013 Report

Content

This attachment contains a description of the atmospheric transport, dispersion and deposition modelling (ATDM) of air concentration over Japan that has been used by the Committee. It includes details of the latest source term developed by the group of researchers at the Japan Atomic Energy Agency (JAEA) [Terada et al., 2020], the dispersion modelling and the outputs used for the Committee's assessments of doses and how the results of ATDM compare with measurements.

Notes

The designations employed and the presentation of material in this publication do not imply the expression of any opinion whatsoever on the part of the Secretariat of the United Nations concerning the legal status of any country, territory, city or area, or of its authorities, or concerning the delimitation of its frontiers or boundaries.

Information on Uniform Resource Locators (URLs) and links to Internet sites contained in the present publication are provided for the convenience of the reader and are correct at the time of issue. The United Nations takes no responsibility for the continued accuracy of that information or for the content of any external website.

© United Nations, March 2022. All rights reserved, worldwide.

This publication has not been formally edited.

CONTENTS

I. INTRODUCTION

1. The assessment of doses from external exposure to the plume and internal exposure from inhalation of radionuclides in the plume could not be based on the few available environmental measurements of radionuclide concentrations in air. Rather it has been based on an assumed source term and ATDM to estimate radionuclide concentrations in air resulting from the dispersion of released radioactive material in the atmosphere and its deposition on to the ground.

2. The concentrations of radionuclides in air were obtained from the assumed source term and ATDM in two ways: *(a)* directly from the ATDM; and *(b)* in combination with data on measured levels of the deposition density of radionuclides. The methods used to assess doses (both from external exposure and from internal exposure due to intakes by inhalation) from the estimated concentrations of radionuclides in the air are described in attachment A-10.

II. MEASUREMENT DATA

3. There have been extensive measurements of the levels of radioactive material in the environment across Japan following the Fukushima Daiichi nuclear power station (FDNPS) accident after 2013. JAEA has collected environmental monitoring data published by various organizations related to the accident, including air dose rate, and radioactive concentration (ground surface, soil, seawater, marine soil, river water, river sediment, groundwater and food), These data sets form the Environment Monitoring Database (EMDB) which is available to the public through an online website [JAEA, WEB]. The data sets and how they have been used by the Committee are described in more detail in attachments A-5 to A-8.

4. Measurements of concentrations of radionuclides in air over Japan during the release were rather limited, in particular, in the early stages of the accident and in the areas devastated by the tsunami. Further data have been published since the UNSCEAR 2013 Report [UNSCEAR, 2014], in particular concentrations of airborne aerosols at seven locations within the Japanese mainland for each hour of the period from 12 March to 11 May 2011 [DTRA, 2013]. The data were derived from measurements on samples collected by the United States Department of Defense (DoD) and the United States Department of Energy (DOE) at or near locations where DoD-affiliated individuals worked or lived. Aside from this new source of measurement information, additional information about the levels of radionuclides in the air and deposited on the ground has come from reanalysis of monitoring data collected at the time and from the application of some novel analysis methods. Specifically, concentrations of different radionuclides in the air in the early stage of the FDNPS accident have been estimated at several monitoring posts in Fukushima Prefecture from pulse height distributions measured with sodium iodide scintillation detectors [Hirayama et al., 2015; Moriizumi et al., 2019; Terasaka et al., 2016]. In addition, concentrations of ^{137}Cs and ^{129}I (from which levels of ^{131}I can be inferred) in air at ground-level in the Fukushima and Kanto areas have been and continue to be derived from an analysis of filter-tapes of air pollution stations (for monitoring suspended particulate matter) [Ebihara et al., 2019; Oura et al., 2015; Tsuruta et al., 2014; Tsuruta et al., 2018], although it should be noted that only iodine in particulate form will have been collected on these filter tapes. The latest version of the data set produced by this work includes information on ^{137}Cs levels for 101 locations and on ^{131}I for 4 locations. The available measurement information is summarized in table A-9.1.

Table A-9.1. Summary of measurements of concentrations of radionuclides in air over Japan

Reference	*Measurement type*	*Locations*	*Radionuclides*
[Hirayama et al., 2013]	$LaBr_3$–Detector	Fukushima Prefecture, 6 measurement points (Adatara SA, Motomiya IC, Koriyama-higasi IC, Miharu PA, Funahiki-Miharu IC, Abukuma-kogen SA)	^{132}Te, ^{131}I, ^{132}I, ^{133}Xe, ^{136}Cs, ^{134}Cs
[Hirayama et al., 2015]	Automatic NaI(Tl)-station	Fukushima Prefecture, 9 monitoring stations (Hirono Town Futatunuma, Fukushima City Momijiyama, Okuma Town Oono, Futaba Town Koriyama, Futaba Town Yamada, Okuma Town Mukaihata, Okuma Town Minamidai, Okuma Town Ottozawa, Naraha Town Shoukan)	^{131}I
[Hirayama et al., 2017]	Automatic NaI(Tl)-station	Fukushima Prefecture, 8 monitoring stations (Futaba Town Yamada, Okuma Town Mukaihata, Okuma Town Oono, Okuma Town Minamidai, Okuma Town Ottozawa, Naraha Town Shoukan, Hirono Town Futatunuma, Fukushima City Momijiyama)	^{132}Te, ^{131}I, ^{132}I, ^{133}I, ^{135}Xe, ^{133}Xe, ^{135m}Xe
[KEK, 2015]	Automatic NaI(Tl)-station	Fukushima Prefecture, 8 monitoring stations (Futaba Town Yamada, Okuma Town Mukaihata, Okuma Town Oono, Okuma Town Minamidai, Okuma Town Ottozawa, Naraha Town Shoukan, Hirono Town Futatunuma, Fukushima City Momijiyama)	^{131}I
[Terasaka et al., 2016]	Automatic NaI(Tl)-station	Ibaraki Prefecture, 6 monitoring stations (Muramatsu, Ajigaura, Araji, Ohnuki, Ishikawa, Sugaya)	^{133}Xe, ^{132}Te, ^{131}I, ^{132}I, ^{133}I, ^{137}Cs, ^{134}Cs, ^{136}Cs
[Moriizumi et al., 2019]	Automatic NaI(Tl)-station	Ibaraki Prefecture, 21 monitoring stations (Toyooka, Mawatari, Oshinobe, Yokobori, Hitachinaka, Horiguchi, Hiroura, Kadobe, Funaishikawa, Ebisawa, Muramatsu, Ohba, Tsukuriya, Ishigami, Kuji, Isobe, Ajigaura, Araji, Ohnuki, Ishikawa, Sugaya)	^{133}Xe, ^{132}Te, ^{131}I, ^{132}I, ^{133}I
[Fukushima Prefecture, 2020]	Gamma-spectrometric measurement with Ge-detector	Fukushima Prefecture, 14 monitoring stations (very few measurements each)	^{132}Te, ^{131}I, ^{132}I, ^{137}Cs, ^{134}Cs
[Tsuruta et al., 2018]	Filter samples	Fukushima Prefecture, 2 SPM monitoring stations (Futaba Town, Naraha)	^{137}Cs, ^{134}Cs
[Oura et al., 2015]	Filter samples measured with Ge detectors	Several prefectures, 99 SPM monitoring stations	^{137}Cs, ^{134}Cs
[Ebihara et al., 2019]	Filter samples analysed with accelerator mass spectrometry	Tokyo Metropolitan Area, 4 monitoring stations (TIRI, TMU, RIKEN, KNZ)	^{129}I, ^{131}I, ^{137}Cs
[DTRA, 2013]	Filter samples analysed with γ-spectrometry systems	4 monitoring stations (Misawa Air Base, Sendai City (Sendai Airport), Ishinomaki (City of Ishinomaki), Yokoata Air Base)	^{140}Ba, ^{134}Cs, ^{136}Cs, ^{137}Cs, ^{131}I, ^{133}I, ^{140}La, ^{86}Rb, ^{99}Mo, ^{99m}Tc, ^{129}Te, ^{129m}Te, ^{131m}Te, ^{132}Te
[Amano et al., 2012]	Filter samples analysed with γ-spectrometry systems	Chiba Metropolitan Area, one monitoring station (JCAC)	^{134}Cs, ^{136}Cs, ^{137}Cs, ^{131}I, ^{132}I, ^{133}I, ^{132}Te
[Doi et al., 2013]	Filter samples analysed with γ-spectrometry systems	Tsukuba, one monitoring station (NIES)	^{131}I, ^{133}I ^{132}Te, ^{134}Cs, ^{136}Cs, ^{137}Cs, ^{129m}Te, ^{99}Mo
[JAEA, 2013]	Filter samples analysed with γ-spectrometry systems	Filter samples, 3 monitoring station	^{131}I, ^{133}I, ^{132}Te, ^{134}Cs, ^{136}Cs, ^{137}Cs, ^{129m}Te

5. Despite the availability of this measurement information, the number of measurements of concentrations of radionuclides in air, particularly for ^{131}I, was still too limited to be used to estimate doses to the public from external exposure to the radionuclides in the air or from internal exposure from inhalation of airborne radionuclides. Instead, concentrations of radionuclides in the air, and the resulting doses from external and internal exposure, have been estimated using an assumed source term and ATDM to reflect the atmospheric dispersion of the released radioactive material and the measured deposition of radionuclides on to the ground. The measurement information has been used for validating the approach used to estimate concentrations of radionuclides in the air. The methods used to estimate concentrations of radionuclides in the air and the validation comparisons between the modelling results and the measurement data are described in this attachment. Attachment A-10 describes how doses from external and internal exposure to the airborne radionuclides have been calculated from the estimated air concentrations.

III. SOURCE TERM

6. The source term and ATDM used by the Committee to estimate concentrations of radionuclides in the air were those derived by Terada et al. [Terada et al., 2020]. An earlier version of this source term, based on less information [Terada et al., 2012], had been used for the same purposes by the Committee in its UNSCEAR 2013 Report [UNSCEAR, 2014]. Both source terms (and others in the series of refinements that have been made by the same group of researchers) have been derived from the measurement information on concentrations of radionuclides in the air and deposited on the ground using reverse ATDM and optimization of the fit between measurements and modelled values.

7. The source term derived by Terada et al. [Terada et al., 2020] represented a further refinement of the source term estimated in a number of previous studies [Katata et al., 2015], and the ATDM simulation was improved with an optimization method that made use of various measurements, including air concentration, surface deposition, and more recently measured hourly air concentrations of ^{137}Cs derived by analysing suspended particulate matter collected at air pollution monitoring stations [Oura et al., 2015; Tsuruta et al., 2018]. The source term spanned the period 03:00 JST on 12 March to 09:00 JST on 1 April 2011. Details about the source term from Terada et al. [Terada et al., 2020] are given in the following table A-9.2 (which has been reproduced from Terada et al. [Terada et al., 2020]).

Table A-9.2. Updated source term of ^{137}Cs and ^{131}I for the period from 05:00 JST on 12 March to 00:00 JST on 1 April 2011. Release rates are decay corrected at the shutdown time of 14:46 JST on 11 March 2011. (Reproduced from supplementary data of Terada et al. [Terada et al., 2020])

	Release period	*Release rate (Bq/h)*		*Release height (m)*
Start time (JST)	*Duration (h)*	^{137}Cs	^{131}I	
05:00, 12 March	4.0	3.88×10^{12}	4.05×10^{13}	20
09:00	1.0	4.20×10^{12}	4.50×10^{13}	20
10:00	4.0	2.70×10^{12}	2.96×10^{13}	20
14:00	1.0	7.20×10^{13}	5.70×10^{15}	120
15:00	1.0	2.70×10^{14}	4.20×10^{15}	$100 \times 100 \times 100^{a}$
16:00	6.0	1.40×10^{13}	1.19×10^{14}	120
22:00	6.0	3.23×10^{13}	2.31×10^{14}	120
04:00, 13 March	5.0	2.15×10^{13}	2.22×10^{14}	120
09:00, 13 March	3.0	2.60×10^{13}	3.04×10^{14}	120
12:00, 13 March	1.0	3.80×10^{13}	4.48×10^{14}	120
13:00, 13 March	2.0	4.95×10^{13}	6.40×10^{14}	120
15:00, 13 March	8.0	3.00×10^{13}	3.61×10^{14}	120
23:00, 13 March	3.0	8.20×10^{12}	1.01×10^{14}	120
02:00, 14 March	1.0	6.30×10^{12}	7.81×10^{13}	120
03:00, 14 March	4.0	4.40×10^{12}	5.49×10^{13}	120
07:00, 14 March	4.0	3.50×10^{12}	4.43×10^{13}	120
11:00, 14 March	1.0	1.86×10^{14}	2.30×10^{15}	$100 \times 100 \times 300^{a}$
12:00, 14 March	6.0	1.80×10^{12}	2.33×10^{13}	20
18:00, 14 March	1.0	1.10×10^{12}	1.44×10^{13}	20
19:00, 14 March	1.0	1.00×10^{12}	1.32×10^{13}	20
20:00, 14 March	1.0	1.00×10^{12}	1.40×10^{13}	20
21:00, 14 March	1.0	2.90×10^{13}	3.50×10^{14}	20
22:00, 14 March	1.0	1.20×10^{12}	1.60×10^{13}	20
23:00, 14 March	1.0	1.25×10^{12}	1.80×10^{15}	20
0:00, 15 March	1.0	1.30×10^{12}	1.80×10^{13}	20
01:00, 15 March	1.0	6.60×10^{13}	5.20×10^{14}	20
02:00, 15 March	1.0	1.00×10^{14}	3.00×10^{14}	20
03:00, 15 March	1.0	1.40×10^{14}	5.50×10^{14}	20
04:00, 15 March	3.0	1.40×10^{13}	2.00×10^{14}	20
07:00, 15 March	3.0	7.77×10^{13}	1.23×10^{15}	20
10:00, 15 March	1.0	7.90×10^{13}	1.30×10^{15}	20
11:00, 15 March	5.0	1.06×10^{13}	1.54×10^{14}	20
16:00, 15 March	2.0	5.15×10^{13}	5.45×10^{14}	20, 120
18:00, 15 March	2.0	2.60×10^{14}	1.99×10^{15}	20, 120
20:00, 15 March	2.0	7.20×10^{13}	6.80×10^{14}	20, 120
22:00, 15 March	1.0	3.40×10^{14}	2.10×10^{16}	20, 120
23:00, 15 March	1.0	1.90×10^{13}	2.90×10^{14}	20, 120

	Release period	*Release rate (Bq/h)*		*Release height (m)*
Start time (JST)	*Duration (h)*	^{137}Cs	^{131}I	
00:00, 16 March	1.0	1.27×10^{13}	2.80×10^{14}	20, 120
01:00, 16 March	5.0	6.64×10^{12}	2.66×10^{14}	20, 120
06:00, 16 March	3.0	1.83×10^{13}	3.23×10^{14}	20
09:00, 16 March	2.0	2.60×10^{14}	2.70×10^{15}	20
11:00, 16 March	1.0	1.20×10^{13}	2.10×10^{14}	20
12:00, 16 March	1.0	1.50×10^{13}	2.29×10^{14}	20
13:00, 16 March	1.0	2.90×10^{13}	4.44×10^{14}	20
14:00, 16 March	1.0	5.00×10^{13}	7.69×10^{14}	20
15:00, 16 March	15.0	6.20×10^{13}	9.47×10^{14}	20
06:00, 17 March	15.0	3.10×10^{13}	5.08×10^{14}	20
21:00, 17 March	3.0	3.00×10^{13}	5.10×10^{14}	20
00:00, 18 March	5.0	2.10×10^{13}	3.60×10^{14}	20
05:00, 18 March	3.0	8.15×10^{13}	2.10×10^{15}	20
08:00, 18 March	5.0	1.98×10^{13}	2.88×10^{15}	20
13:00, 18 March	5.0	9.71×10^{13}	2.89×10^{15}	20
3/18 18:00, 18 March	11.0	5.80×10^{13}	1.50×10^{15}	20
05:00, 19 March	10.0	9.90×10^{13}	1.91×10^{15}	20
15:00, 19 March	19.0	6.48×10^{12}	7.69×10^{13}	20
10:00, 20 March	10.0	2.18×10^{13}	3.37×10^{14}	20
20:00, 20 March	12.0	3.70×10^{13}	2.25×10^{14}	20
08:00, 21 March	4.0	4.38×10^{12}	1.03×10^{14}	20
12:00, 21 March	4.0	4.10×10^{11}	1.18×10^{14}	20
16:00, 21 March	5.0	2.80×10^{12}	5.10×10^{13}	20
21:00	26.0	1.07×10^{12}	2.92×10^{14}	20
23:00, 22 March	25.0	2.24×10^{12}	5.74×10^{14}	20
00:00, 24 March	24.0	6.31×10^{11}	5.13×10^{13}	20
00:00, 25 March	35.0	2.20×10^{12}	1.26×10^{14}	20
11:00, 26 March	47.0	6.91×10^{11}	6.46×10^{13}	20
10:00, 28 March	35.0	3.00×10^{12}	1.21×10^{13}	20
21:00, 29 March	14.0	5.87×10^{12}	4.26×10^{13}	20
11:00, 30 March	13.0	4.32×10^{13}	2.66×10^{14}	20
00:00, 31 March	22.0	2.70×10^{12}	7.95×10^{13}	20
22:00, 31 March	2.0	8.91×10^{11}	5.30×10^{12}	20

[a] Volume source dimension in the directions *x*, *y*, and z resulting from a hydrogen explosion.

IV. ATMOSPHERIC TRANSPORT, DISPERSION AND DEPOSITION MODELLING SIMULATIONS OF AIRBORNE RADIOACTIVITY

8. Table A-9.3 provides details of the model parameters used in the recent ATDM carried out by Terada et al. [Terada et al., 2020] and used by the Committee for its updated dose assessment, and provides a comparison with the parameters and assumptions made in the earlier source term and ATDM used by the Committee in the UNSCEAR 2013 Report [UNSCEAR, 2014].

9. Unlike in the UNSCEAR 2013 Report [UNSCEAR, 2014], the Committee has used the same ATDM of Terada et al. [Terada et al., 2020] to estimate concentrations of radionuclides in the air as was used to derive the source term from the available measurement data using reverse modelling. The ATDM used by Terada et al. was that in WSPEEDI, with a new meteorological model (WRF) and data assimilation method [Terada et al., 2020]. ATDM results have been provided to the Committee for two nested grids, the finer grid covering most of Fukushima Prefecture with a grid size of 1×1 km^2 (local model), the coarse grid covering Fukushima Prefecture and all neighbouring prefectures with a grid size of 3×3 km^2 (regional model) [Terada et al., 2020]. ATDM results have been provided for the radionuclides ^{131}I, ^{132}Te, ^{134}Cs and ^{137}Cs.

Table A-9.3. Description of atmospheric transport, dispersion and deposition modelling used in the UNSCEAR 2013 Report and in this update

Model parameter/assumption	*UNSCEAR 2013 Report [UNSCEAR, 2014]*	*Update – this study (local model)*	*Update – this study (regional model)*
Source term	[Terada et al., 2012]	[Terada et al., 2020]	[Terada et al., 2020]
ATDM-meteorological model	NOAA(HYSPLIT) - GDAS[a]	WSPEEDI-WRF	WSPEEDI-WRF
Area	approx. 3 000 × 2 000 km	36.310° N – 38.024° N 139.384° E – 141.506° E	34.416° N – 39.553° N 137.805° E – 143.989° E
Height range	0–>10 km	0–9 306 m	0–9 306 m
# of grid cells	601 × 401	187 × 187	187 × 187
# of height levels	56 layers; 10 within the lowest 1 km	28	28
Grid size	5×5 km^2	1×1 km^2	3×3 km^2
Time period (JST)	03:00, 12 March 2011 to 06:00, 4 April 2011	16:00, 12 March 2011 to 15:00, 31 March 2011	16:00, 11 March 2011 to 15:00, 31 March 2011
Time resolution	3 hours	1 hour	1 hour
Radionuclides	^{137}Cs, ^{136}Cs, ^{134}Cs, ^{131}I, ^{132}I, ^{133}I (for all iodines: separately for gaseous (elemental and organic combined) and particulate forms), ^{132}Te, ^{133}Xe	^{137}Cs, ^{134}Cs, ^{132}Te, ^{131}I (total + separately for 3 iodine forms (elemental, organic, particulate))	^{137}Cs, ^{134}Cs, ^{132}Te, ^{131}I (total + separately for 3 iodine forms (elemental, organic, particulate))
Results	- Air concentration - Total deposition	- Precipitation intensity - Wind speed (U-/V-direction) - Air concentration - Total deposition - Dry deposition - Wet deposition - Fog deposition	- Precipitation intensity - Wind speed (U-/V-direction) - Air concentration - Total deposition - Dry deposition - Wet deposition - Fog deposition

[a] United States National Oceanic and Atmospheric Administration (NOAA) ATDM (Hybrid Single-Particle Lagrangian Integrated Trajectory Model (HYSPLIT)) combined with Global Data Assimilation System (GDAS) meteorological model.

V. ATMOSPHERIC TRANSPORT, DISPERSION AND DEPOSITION MODELLING: RESULTS FOR CONCENTRATIONS OF RADIONUCLIDES IN THE AIR

10. Figures A-9.I to A-9.IV (left side: local model, right side: regional model) show the calculated time-integrated concentrations of ^{131}I (total of all three forms), ^{132}Te, ^{134}Cs and ^{137}Cs in air for the period from 11 March to 31 March 2011, as derived from the time-dependent air concentrations calculated by the ATDM of [Terada et al., 2020]. These maps demonstrate that a significant proportion of the releases of radionuclides to atmosphere were dispersed over the ocean.

Figure A-9.I. Time-integrated concentration of total ^{131}I in air for the period from 11 March to 31 March 2011, derived from the atmospheric transport, dispersion and deposition modelling results of [Terada et al., 2020]

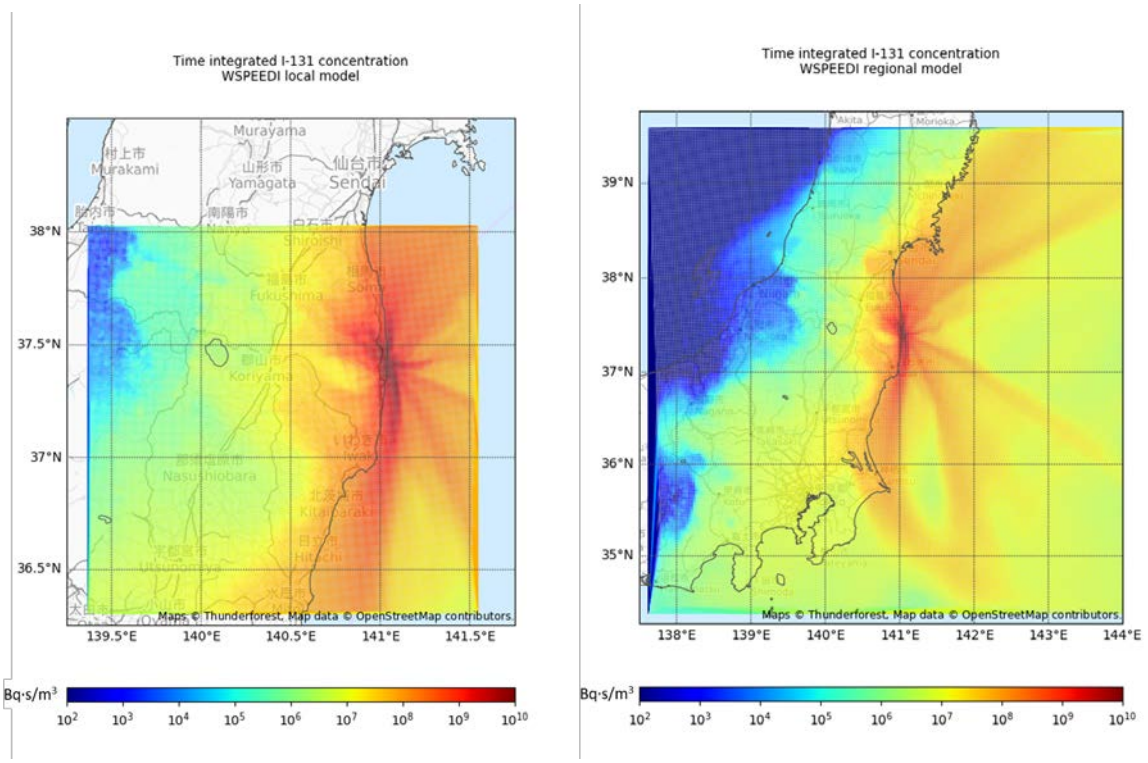

Figure A-9.II. Time-integrated concentration of ^{132}Te in air for the period from 11 March to 31 March 2011, derived from the atmospheric transport, dispersion and deposition modelling results of [Terada et al., 2020]

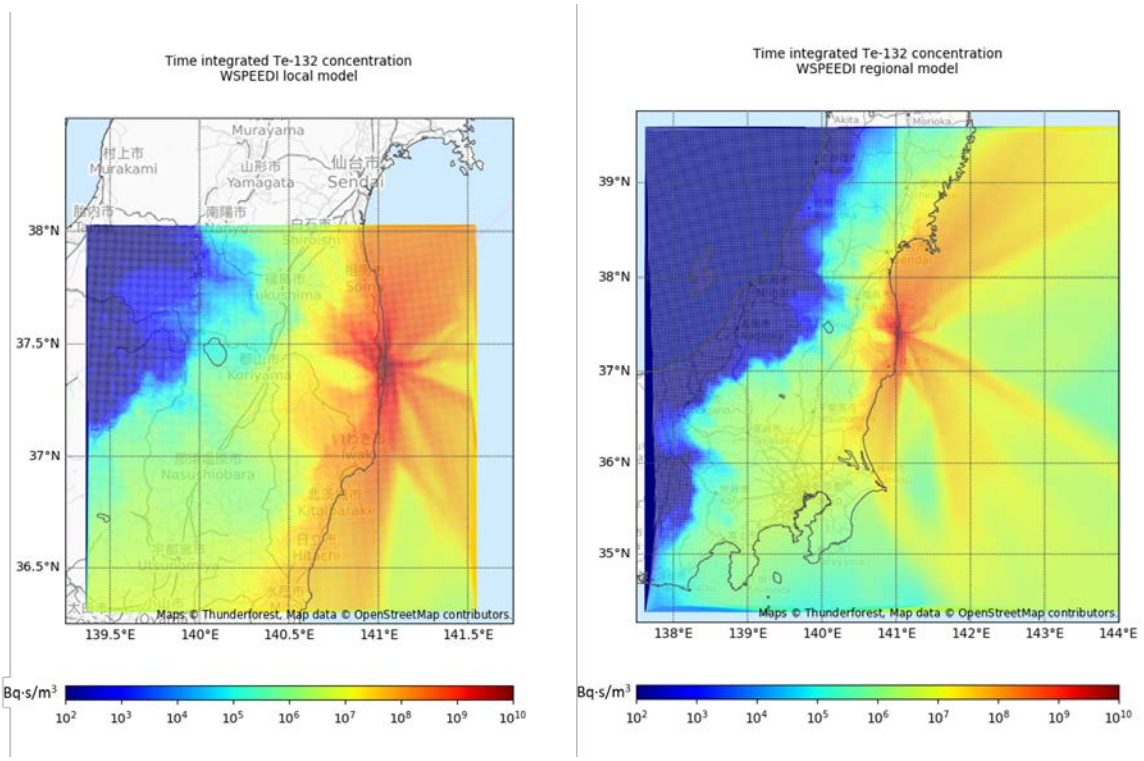

Figure A-9.III. Time-integrated concentration of ^{134}Cs in air for the period from 11 March to 31 March 2011, derived from the atmospheric transport, dispersion and deposition modelling results of [Terada et al., 2020]

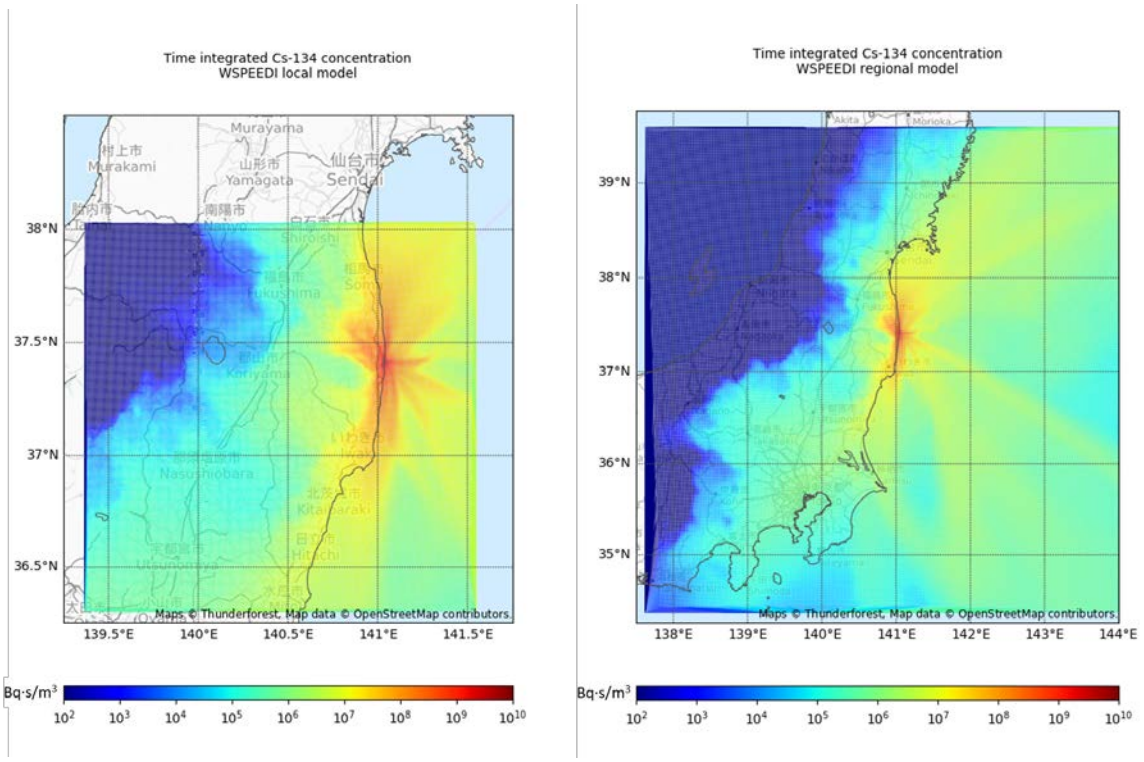

Figure A-9.IV. Time-integrated concentration of ^{137}Cs in air for the period from 11 March to 31 March 2011, derived from the atmospheric transport, dispersion and deposition modelling results of [Terada et al., 2020]

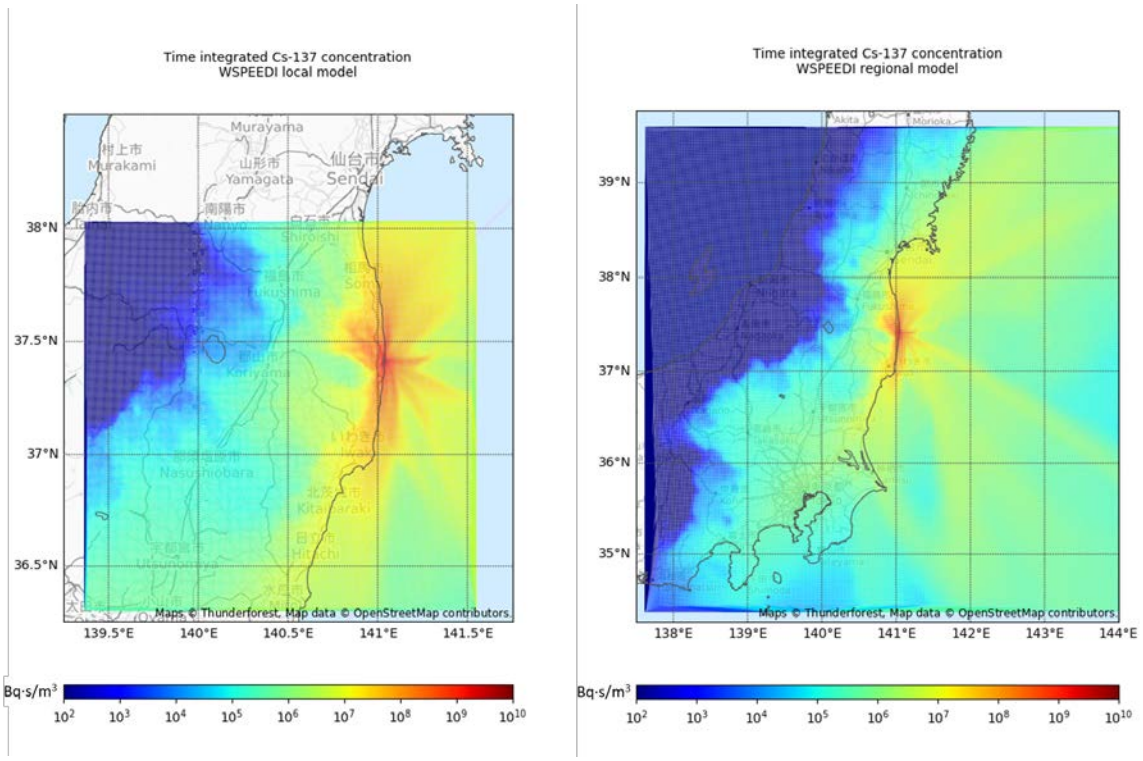

VI. COMPARISON OF MODELLED AND MEASURED DEPOSITION LEVELS

11. The ATDM results can be compared with measured levels of radionuclides in the environment to validate the model. Figures A-9.V and A-9.VI show a comparison of the ATDM results for the deposition densities of ^{137}Cs and ^{131}I with the measurements from the JAEA EMDB [Saito and Onda, 2015]. On average, the ATDM model better reproduces the deposition density of ^{137}Cs than that of ^{131}I. Perfect matching of modelled and measured deposition levels would result in a diagonal line as shown in figure A-9.V. For ^{137}Cs, the data in figure A-9.V (left side) are evenly distributed around such a line, with 49% of the data points below and 51% above. For ^{131}I, many more (83%) data points are below the line indicating that the ATDM has underestimated the measured deposition levels. This finding is also supported by the median value of the ratio of modelled and measured deposition densities, which is 1.05 for ^{137}Cs and only 0.33 for ^{131}I (geometric mean is 0.86 for ^{137}Cs and 0.64 for ^{131}I). For ^{137}Cs, about 34% of the modelled deposition densities are within a factor of 2 of the measured values (30% for ^{131}I), about 68% within a factor of 5 (65% for ^{131}I) and about 84% within a factor of 10 (84% for ^{131}I). It is difficult to assess the uncertainty of the model predictions of air concentration from this comparison of deposition data, as the deposition model in the ATDM and the uncertainty in the meteorological data regarding precipitation bring in significant additional uncertainty.

12. It can be seen from figure A-9.VI that there are significant differences in the performance of the ATDM depending on the location: while the modelled deposition densities match the measurements quite well along the coast (indicated by green colours; especially visible for ^{131}I), the model underestimate deposition densities to the north-west of FDNPS, in the area of Fukushima City, in the Nakadori valley and in the western parts of Fukushima Prefecture (blue

colours; in all these areas the underestimation is larger for ^{131}I than for ^{137}Cs). Especially for ^{137}Cs, the model tends to overestimate the deposition densities in the mountainous regions west of FDNPS and also south of FDNPS (orange colours).

Figure A-9.V. Comparison of modelled and measured deposition levels of ^{137}Cs and ^{131}I

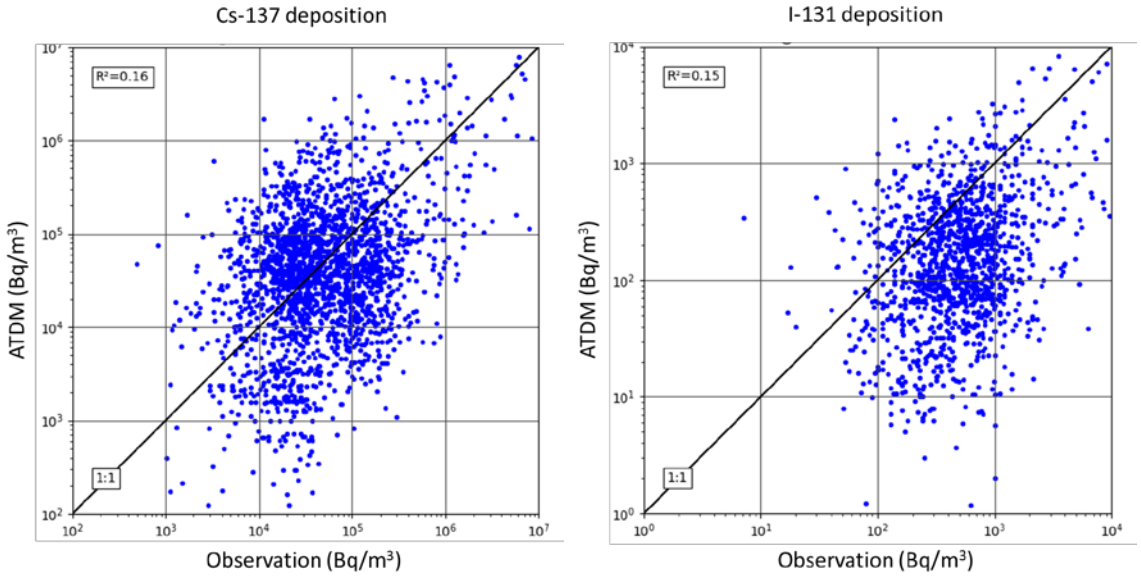

Figure A-9.VI. Ratio of modelled and measured deposition levels for ^{137}Cs (left side) and ^{131}I (right side)

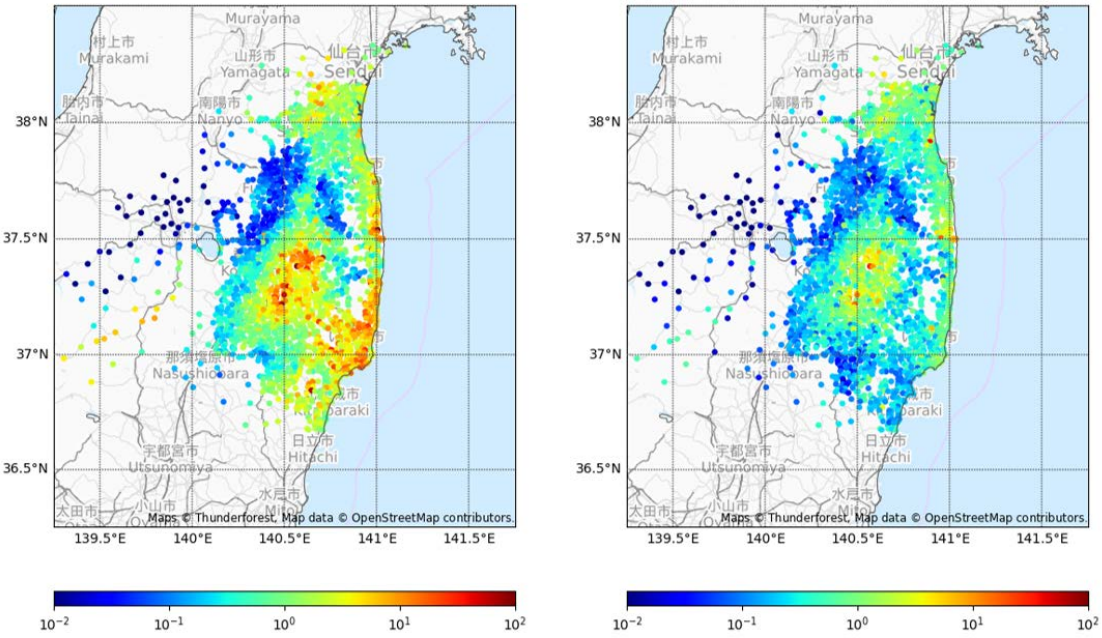

VII. ESTIMATION OF CONCENTRATIONS OF RADIONUCLIDES IN AIR FOR DOSE ASSESSMENT

13. The Committee has used two different methods to estimate concentrations of radionuclides in air for the purposes of assessing doses to the public. The first method was based solely on the results of the ATDM provided by Terada et al. [Terada et al., 2020]. This approach was used for estimating air concentrations in areas of Fukushima Prefecture that were evacuated, because, when estimating doses to those members of the public who were evacuated, information was needed on the concentration of radionuclides in the air as a function of time.

14. The second method was based on the estimated time-integrated concentrations in air derived from the measured deposition densities of radionuclides by dividing by the ratio (the "bulk deposition velocity") of the deposition density to the time-integrated concentration in air estimated from the ATDM results as a function of location. While the estimates of radionuclide concentrations in air and deposition densities of radionuclides provided by the assumed source term and ATDM simulations at any specific location are associated with significant uncertainties, the ratios of these two estimates are much less so. In particular, the ratios are relatively insensitive to the absolute magnitude and temporal pattern of the estimated release of the radioactive material, which is associated with much uncertainty. The main uncertainties in these ratios result from uncertainties in the parameters that describe wet and dry deposition. The Committee used such location-dependent ratios, derived from the ATDM analyses, to infer time-integrated radionuclide concentrations in air from the measured deposition densities of radionuclides in all regions of Japan except in the evacuated areas.

15. The "bulk deposition velocities" were estimated from the ATDM results for the radionuclides in the plume and deposited on the ground as a function of time and location, using the local model of Terada et al. (with a spatial resolution of 1 × 1 km) within Fukushima Prefecture; in other prefectures, average values for the "bulk deposition velocities" using the regional model (with a spatial resolution of 3 × 3 km) were used. The "bulk deposition velocities" applied were based on the ratios of the estimated time-integrated activity concentrations in air to the deposition densities of the radionuclides. This approach was applied to non-evacuated settlements of Fukushima Prefecture and the rest of Japan.

16. The ATDM results provided by Terada et al. include time-dependent concentrations in air and deposition densities for the radionuclides ^{132}Te, ^{131}I, ^{134}Cs and ^{137}Cs. For ^{131}I, three chemical forms have been considered: inorganic particulate, elemental vapour and organic, using the constant ratios, based on experimental and other evidence, of 0.5 for $^{131}I_{particulate}/^{131}I_{total}$, 0.2 for $^{131}I_{elemental}/^{131}I_{total}$ and 0.3 for $^{131}I_{organic}/^{131}I_{total}$. Concentrations in air and deposition densities of ^{132}I were derived by assuming it to be in secular equilibrium with its parent, ^{132}Te (a reasonable assumptions given its much shorter half-life of 2.3 hours compared to the half-life of ^{132}Te of 3.2 days). The short-lived radionuclide ^{133}I was also not considered in the ATDM model from Terada et al. [Terada et al., 2020], and thus the activity concentration in air of ^{133}I had to be estimated from the calculated concentrations of ^{131}I in air by applying a time-dependent (to consider the different half-lives of these iodine isotopes) radionuclide ratio based on the ^{133}I:^{131}I ratio at 14:46 on 11 March 2011 from Nishihara et al. [Nishihara et al., 2012]. The fractions of ^{132}I and ^{133}I in different physico-chemical forms (particulate, elemental and organic iodine) were assumed to be the same as those for ^{131}I. Other shorter lived radionuclides (e.g., ^{129}Te, ^{129m}Te, ^{131m}Te, ^{135}I, ^{136}Cs) have not been included; their contribution to the total dose from inhalation would be small in comparison to the radionuclides that have been included (see e.g., [Ohba et al., 2017]). It was not possible to estimate the air concentrations of noble gases,

specifically of ^{133}Xe, from the ATDM results; the implications of this for the assessment of doses is addressed in attachment A-10.

17. The results of the estimation of concentration of radionuclides in air using the deposition scaling approach are illustrated in the following four figures. Concentrations of radionuclides in air – as shown in figures A-9.VII and A-9.VIII for ^{137}Cs and ^{131}I, respectively – were derived from the deposition measurement data from the JAEA EMDB data sets [Saito and Onda, 2015], in particular, the 2,200-location soil deposition data set for ^{137}Cs (see attachments A-6 to A-8). Bulk deposition velocities – as shown in figures A-9.IX and A-9.X – were derived from the results of the ATDM local model by calculating the ratio of deposition density to time-integrated concentration in air.

Figure A-9.VII. Concentration in air for ^{137}Cs (time-integrated) estimated from deposition measurements using the deposition scaling approach

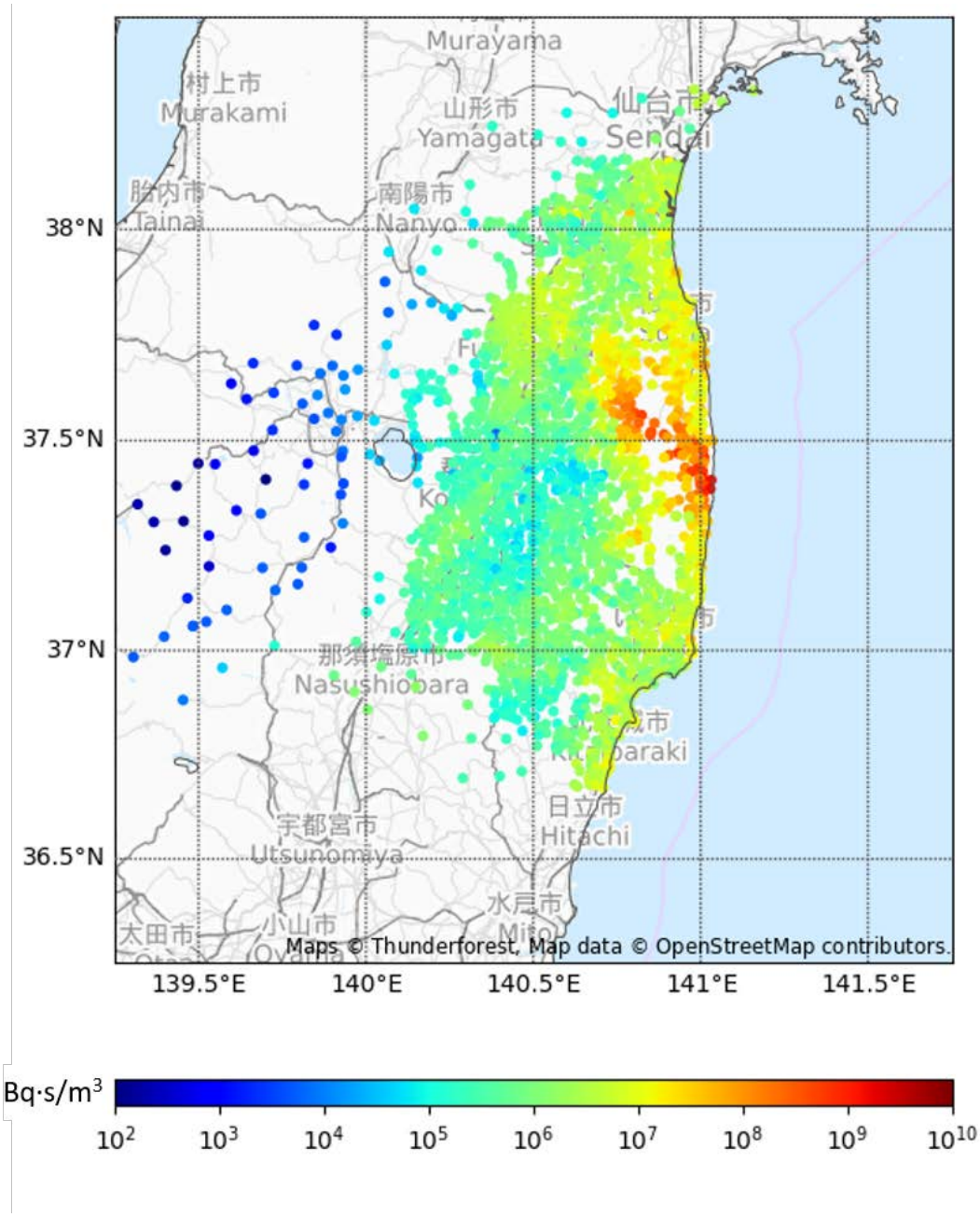

Figure A-9.VIII. Concentration in air for ^{131}I (time-integrated) estimated from deposition measurements using the deposition scaling approach

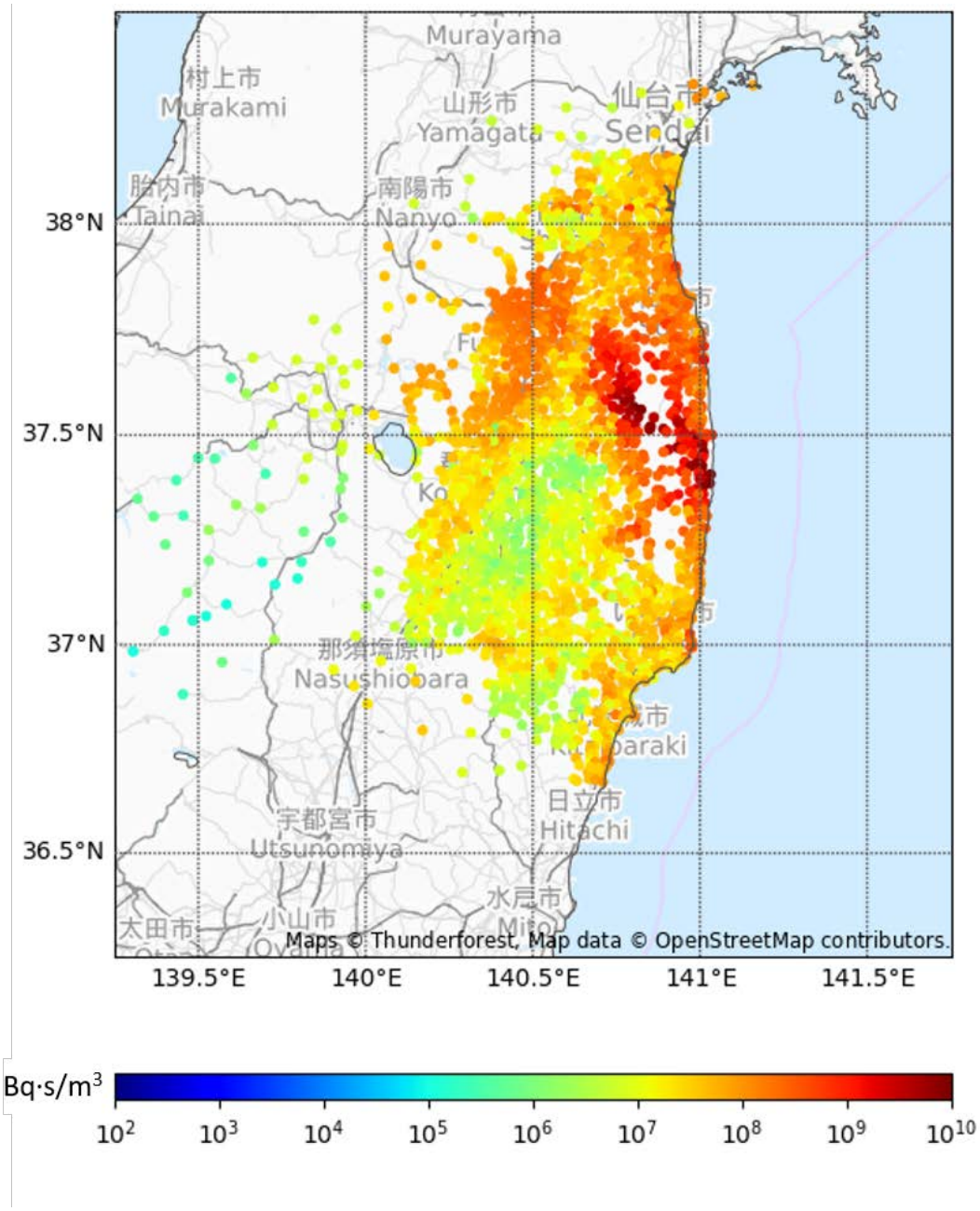

Figure A-9.IX. Bulk deposition velocity for ^{137}Cs estimated from atmospheric transport, dispersion and deposition modelling (i.e., ratio of the modelled deposition density to the modelled time-integrated concentration in air)

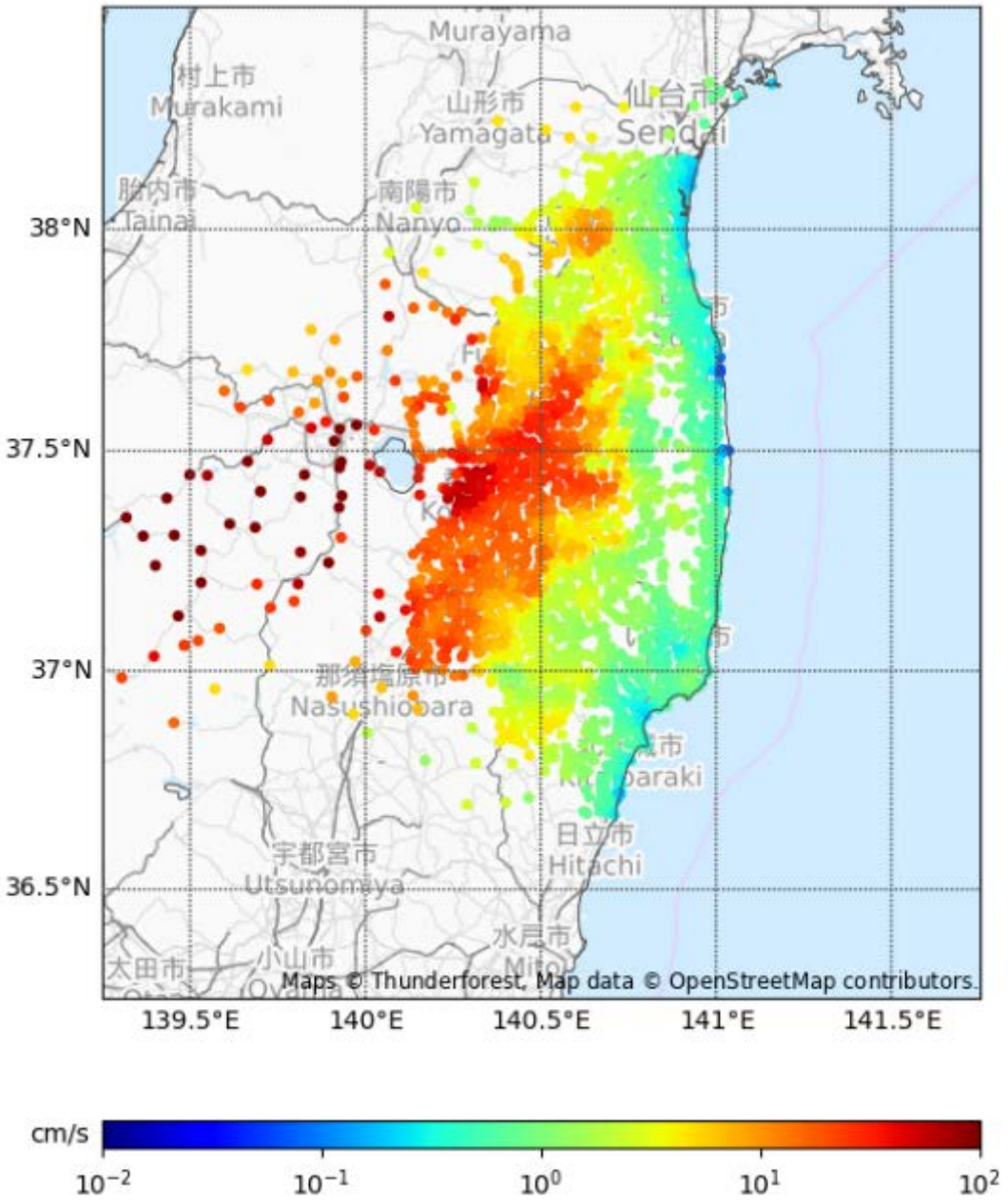

Figure A-9.X. Bulk deposition velocity for ^{131}I estimated from atmospheric transport, dispersion and deposition modelling (i.e., ratio of the modelled deposition density to the modelled time-integrated activity concentration in air)

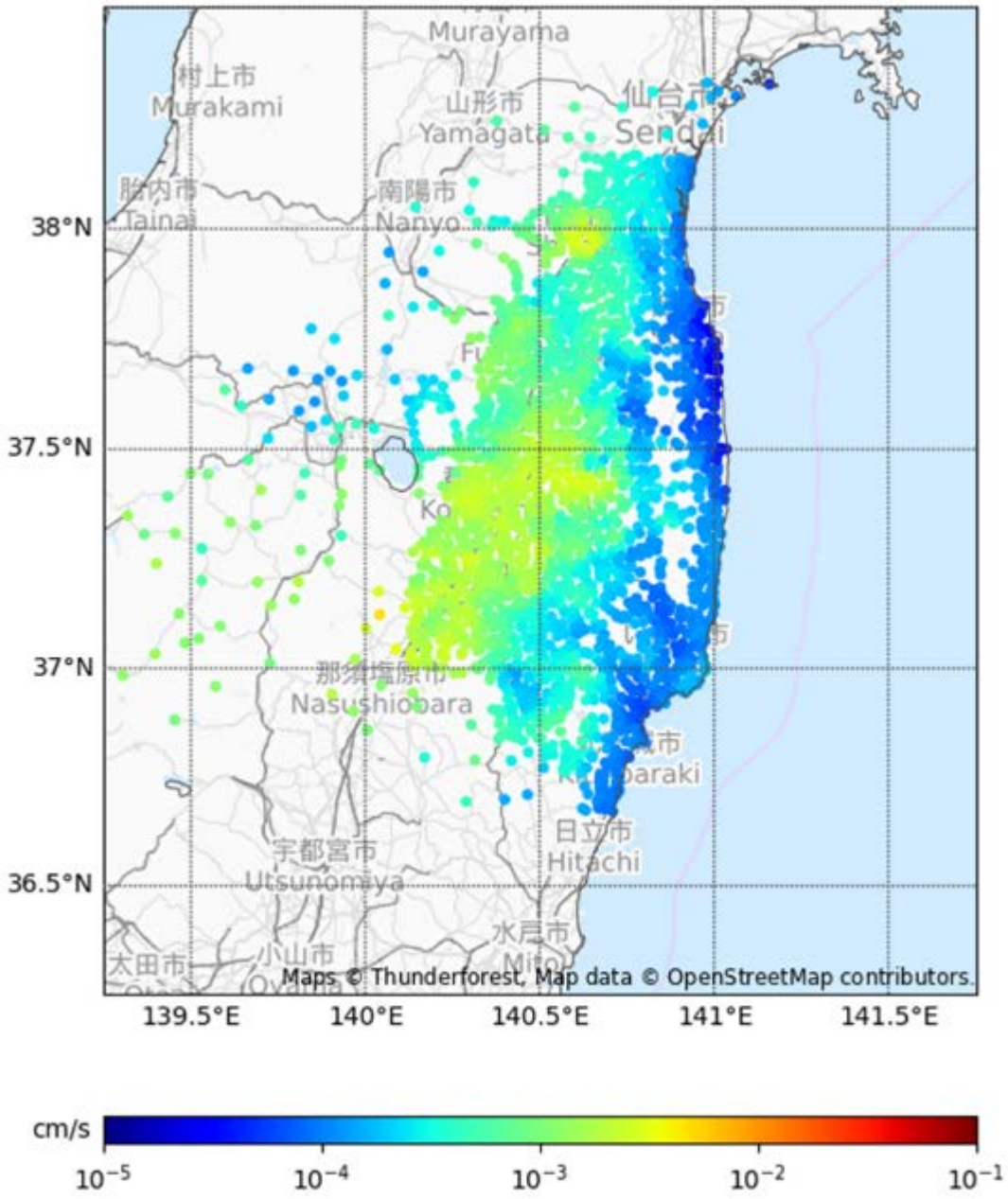

VIII. COMPARISON OF MODELLED AND MEASURED AIR CONCENTRATION FOR ^{137}CS

18. A comparison is made in this section between modelled and measured time-integrated concentrations of ^{137}Cs in air over the period when the main releases from the FDNPS accident occurred (12–22 March 2011). The modelled air concentrations used in the comparison have been derived using two different approaches (directly from ATDM or indirectly using the deposition scaling approach).

19. Time dependent, concentrations of ^{137}Cs (and also of ^{129}I, from which levels of ^{131}I can be inferred) in air at ground-level in Fukushima Prefecture and several other prefectures (Chiba, Ibaraki, Kanagawa, Miyagi, Niigata, Saitama and Yamagata), and in the larger Tokyo Metropolitan Area have been measured (and are still being measured in ongoing research projects) from analyses of filter-tapes of air pollution stations for monitoring suspended particulate matter [Ebihara et al., 2019; Oura et al., 2015; Tsuruta et al., 2014; Tsuruta et al., 2018]; it should be noted, however, that only iodine in particulate form would have been collected on the filter tapes. The latest version of the data set includes information on ^{137}Cs levels for 101 locations, with 23 located within, or close to the border of, Fukushima Prefecture (see figure A-9.XI). Only measurements at these 23 locations have been considered in the comparison. No other measurements of ^{137}Cs in air within the Fukushima Prefecture are known to the Committee that provide a continuous time series over the full period where the main releases of the FDNPS accident occurred (12–22 March 2011). Only with such "complete" time series of measurements can meaningful comparisons be made between modelled and measured air concentrations. There were also two locations within Fukushima Prefecture where measurements of ^{131}I in air are available, but these did not cover the time periods of interest for the dose assessment.

Figure A-9.XI. Locations within or close to the border of Fukushima Prefecture where ^{137}Cs air concentrations have been measured

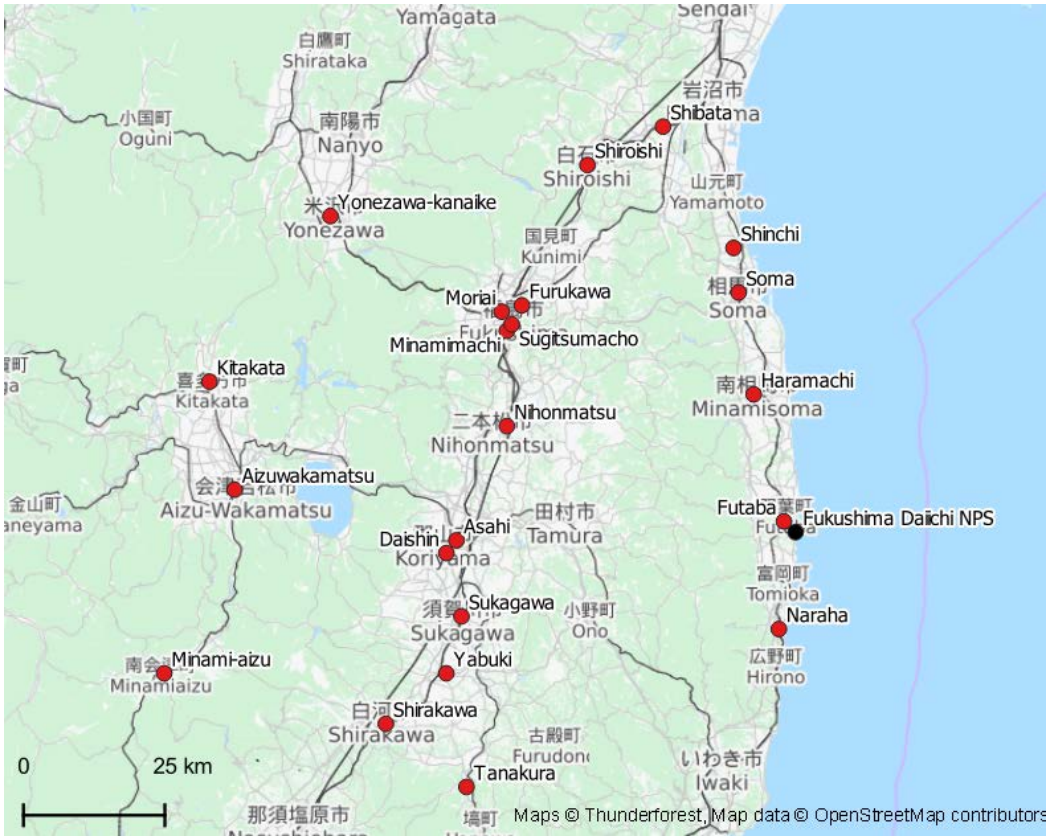

20. A comparison of measured and modelled ^{137}Cs time-integrated concentrations in air at each of the 23 locations within or close to Fukushima Prefecture is provided in table A-9.4. The time-integrated air concentrations estimated from ATDM using deposition scaling are within a factor of two of the measured time-integrated air concentration at six out of the 23 monitoring locations, while this is the case for only three of the monitoring locations if the time-integrated air concentrations estimated directly using ATDM are used. Similarly, time-integrated air concentrations estimated using deposition scaling are within factors of five and ten of the measured air concentrations at 13 and 17 monitoring locations, respectively, whereas the

numbers are 6 and 16, respectively, for time-integrated air concentrations estimated directly using ATDM. The time-integrated concentrations estimated directly by ATDM are higher at some locations than the measured concentrations and lower at others, but are generally lower by large factors (an order of magnitude and more) at the lower concentrations; at higher concentrations (3×10^6 Bq s/m^3 and above), the ATDM estimates are more likely to be higher than the measured concentrations by factors of a few. The concentrations estimated using ATDM and deposition scaling also tend to be lower than the measured concentrations at the lower concentrations, but provide a much closer match to the measurements at higher concentrations. This comparison confirms that the deposition scaling approach provides a generally better estimate of the time-integrated air concentration of ^{137}Cs. As the measurements are not uniformly distributed across Fukushima Prefecture and their number is still relatively limited, they cannot be considered as being fully representative for the whole prefecture and thus no general conclusion can be drawn about the extent of any possible over- or underestimation of the time-integrated air concentration derived using ATDM.

Table A-9.4. Comparison of modelled and measured concentrations of ^{137}Cs in air (time-integrated)

No.	*Location*	*^{137}Cs measurement (Bq s/m^3)*	*^{137}Cs concentrations derived directly from ATDM (Bq s/m^3)*	*^{137}Cs concentration derived from ATDM and deposition scaling (Bq s/m^3)*
1	Aizuwakamatsu	1E+05	8E+02	8E+03
2	Asahi	2E+06	2E+05	2E+05
3	Daishin	2E+06	2E+05	8E+05
4	Furukawa	2E+06	3E+05	5E+06
5	Futaba Town	2E+08	1E+09	2E+08
6	Haramachi	2E+07	4E+07	3E+07
7	Kitakata	1E+05	4E+02	9E+03
8	Minami-aizu	4E+05	2E+04	2E+04
9	Minamimachi	2E+06	2E+05	5E+06
10	Moriai	2E+06	2E+05	5E+06
11	Muikamachi	1E+03	8E+03	2E+04
12	Naraha	7E+07	2E+08	1E+07
13	Nihonmatsu	3E+06	1E+05	2E+06
14	Shibata	3E+05	2E+06	2E+06
15	Shinchi	3E+06	2E+07	1E+07
16	Shirakawa	2E+06	2E+05	1E+06
17	Shiroishi	1E+06	7E+05	3E+05
18	Soma	1E+07	2E+07	7E+06
19	Sugitsumacho	2E+06	3E+05	5E+06
20	Sukagawa	3E+06	4E+05	2E+05
21	Tanakura	1E+06	3E+05	2E+06
22	Yabuki	2E+06	4E+05	3E+05
23	Yonezawa-kanaike	5E+05	4E+03	8E+04

21. A comparison of modelled and measured air concentrations is also shown in figure A-9.XII; modelled concentrations based directly on ATDM are shown as red triangles and those based on deposition scaling as blue circles. The figure shows the generally better agreement with measurements obtained using deposition scaling, with estimates distributed both above and below the corresponding measured values. On the other hand, using ATDM directly to estimate time-integrated air concentrations, results in estimates that are less close to the measurements and, at the higher air concentrations, generally higher than the measured values. At lower air concentrations neither method provides a good fit with the measurements, with estimated values being generally below the measurements.

Figure A-9.XII. Comparison of modelled and measured concentration of ^{137}Cs in air (time-integrated) (red triangles – estimates based directly on atmospheric transport, dispersion and deposition modelling; blue circles – estimates based on atmospheric transport, dispersion and deposition modelling and deposition scaling)

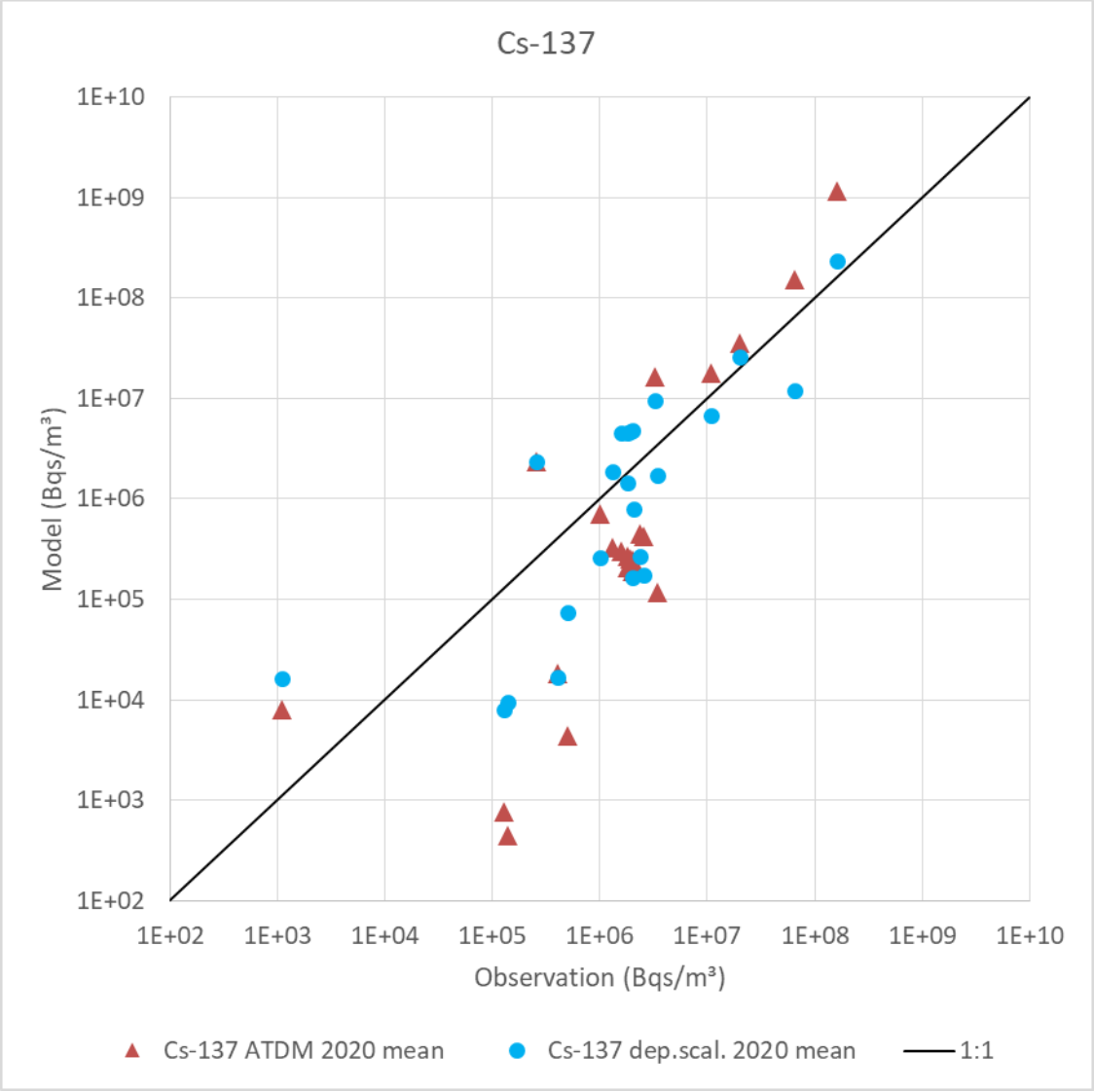

22. The source term and ATDM results have been used directly to provide air concentrations as a function of time for estimating doses to evacuees. A more relevant comparison in this case may be provided by considering the air concentration integrated over a shorter time period and measurements made at monitoring stations in or near to the evacuated locations, specifically Futaba, Haramachi and Naraha. The ratios of the modelled air concentration to the measurements at these three stations integrated over the time period of 12–15 March 2011 (when most of the

evacuations took place) are 1.5, 2.9 and 3.0, respectively. This again shows the overestimation of the modelled air concentrations compared with the measurements at the higher concentrations in these locations. However, it also indicates somewhat better agreement (less than or equal to a factor of three) between the modelled air concentrations and the measurements in the evacuated areas, if consideration is limited to the time periods and locations of greater relevance to the evacuees.

23. Figures A-9.XIII and A-9.XIV show further comparisons of measured and modelled ^{137}Cs concentrations in air (the former of modelled concentrations based directly on ATDM and the latter on concentrations estimated from deposition scaling). The two modelling approaches perform differently (assuming performance is to be assessed by the level of agreement with the air concentration measurements) in different areas of Fukushima Prefecture. Both modelling approaches reproduce the measured (time-integrated) air concentrations of ^{137}Cs quite well along the coast of Fukushima Prefecture. The direct ATDM approach, however, significantly underestimates the concentrations in the central (Nakadori valley) and western parts of the Fukushima Prefecture, sometimes by orders of magnitude; the deposition scaling approach performs better in these areas but differences between the modelled and measured concentrations are evident in the western part of the prefecture.

Figure A-9.XIII. Comparison of modelled and measured concentrations in air for ^{137}Cs (time-integrated) – using the deposition scaling approach

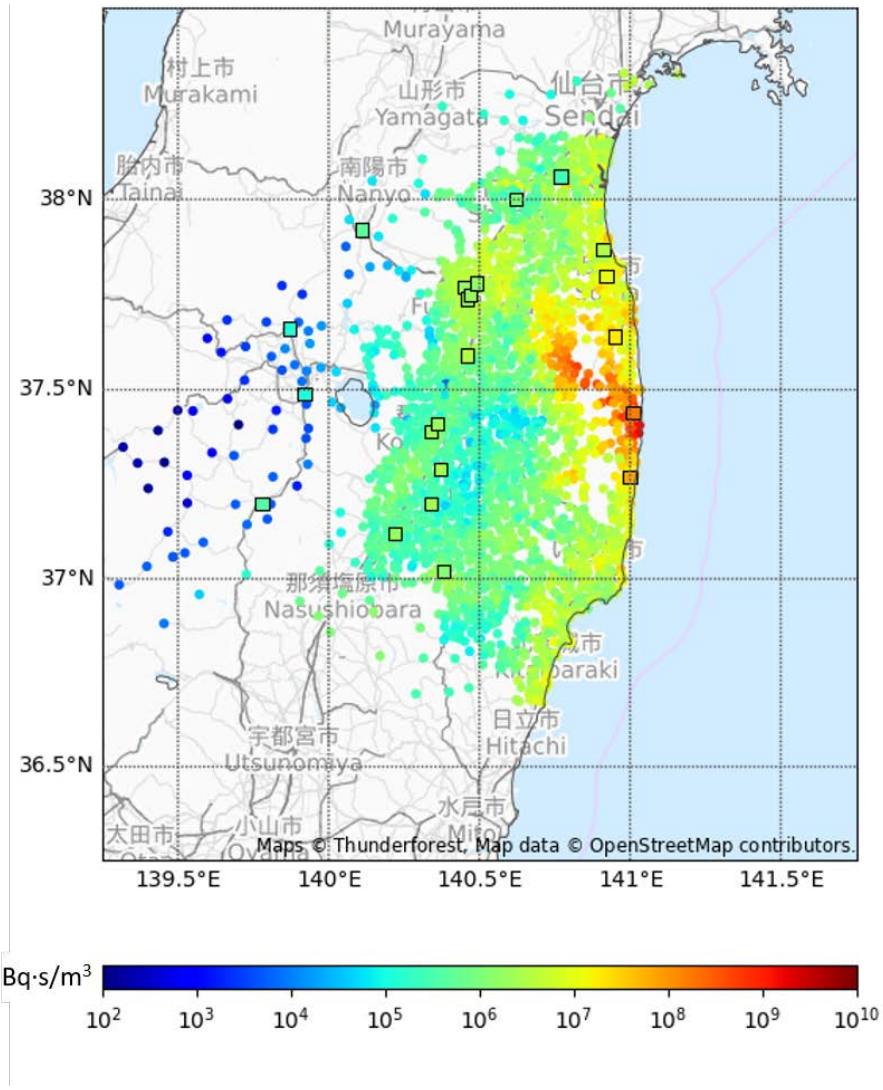

Figure A-9.XIV. Comparison of modelled and measured concentrations in air for ^{137}Cs (time-integrated) using atmospheric transport, dispersion and deposition modelling results directly

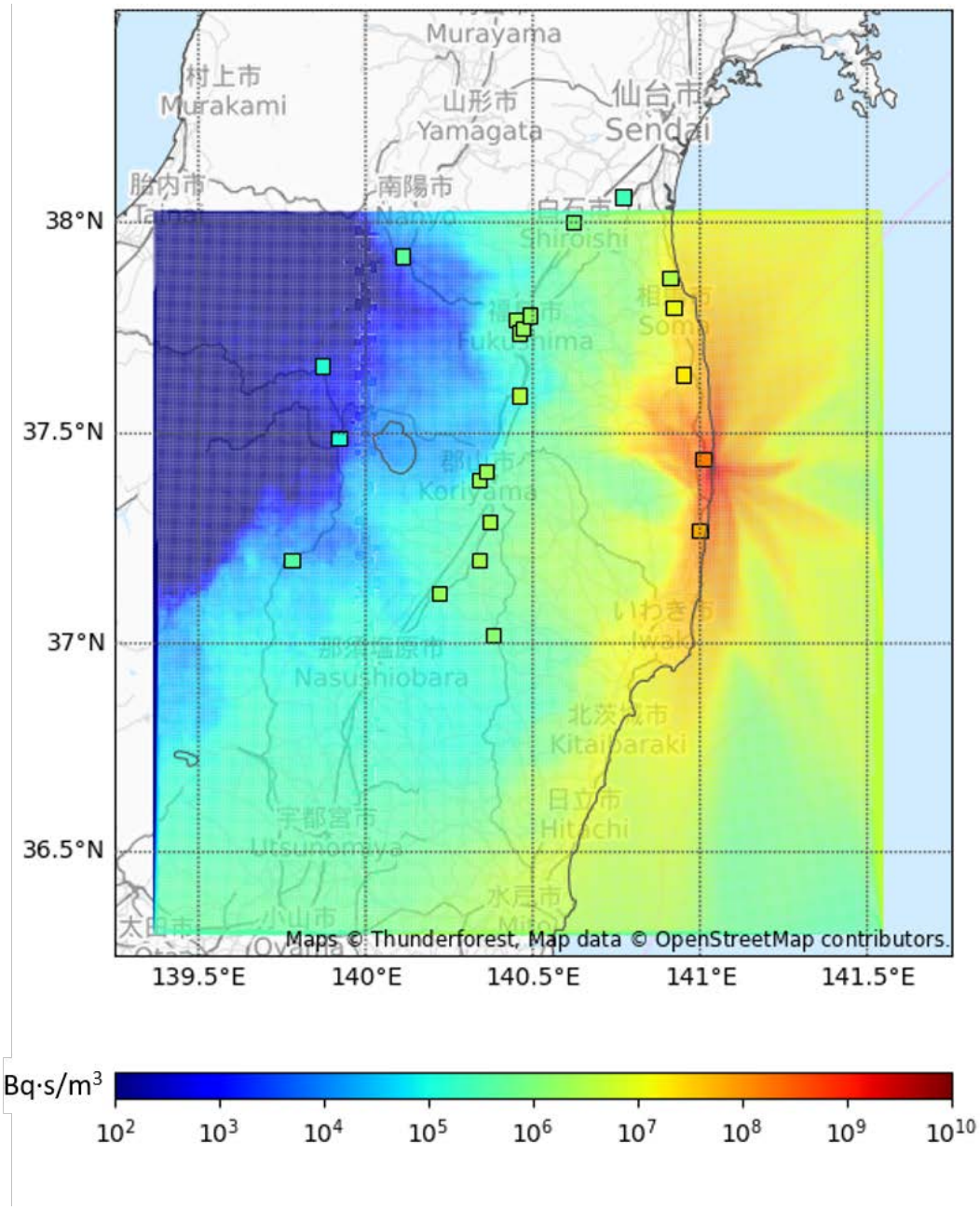

REFERENCES

Amano, H., M. Akiyama, B. Chunlei et al. Radiation measurements in the Chiba Metropolitan Area and radiological aspects of fallout from the Fukushima Dai-ichi Nuclear Power Plants accident. J Environ Radioact 111: 42-52 (2012).

Doi, T., K. Masumoto, A. Toyoda et al. Anthropogenic radionuclides in the atmosphere observed at Tsukuba: characteristics of the radionuclides derived from Fukushima. J Environ Radioact 122: 55-62 (2013).

DTRA. Operation Tomodachi registry: radiation data compendium. DTRA-TR-13-044. Defence Threat Reduction Agency, VA, USA, 2013.

Ebihara, M., Y. Oura, N. Shirai et al. A new approach for reconstructing the ^{131}I-spreading due to the 2011 Fukushima nuclear accident by means of measuring ^{129}I in airborne particulate matter. J Environ Radioact 208-209: 106000 (2019).

Fukushima Prefecture. Results of γ-ray nuclide analysis of airborne dust during emergency monitoring. [Internet] Available from (https://www.pref.fukushima.lg.jp/uploaded/attachment/194216.pdf) on 17 February 2020. (Japanese).

Hirayama, H., H. Matsumura, Y. Namito et al. Estimation of radionuclide concentration in plume using pulse height distribution measured by $LaBr_3$ scintillation detector and its response to radionuclides in plume calculated with egs5. Trans At Energy Soc Japan 12(4): 304-310 (2013). (Japanese).

Hirayama, H., H. Matsumura, Y. Namito et al. Estimation of time history of I-131 concentration in air using NaI(Tl) detector pulse height distribution at monitoring posts in Fukushima Prefecture. Trans At Energy Soc Japan 14(1): 1-11 (2015). (Japanese).

Hirayama, H., H. Matsumura, Y. Namito et al. Estimation of Xe-135, I-131, I-132, I-133 and Te-132 concentrations in plumes at monitoring posts in Fukushima Prefecture using pulse height distribution obtained from NaI(Tl) detector. Trans At Energy Soc Japan 16(1): 1-14 (2017). (Japanese).

JAEA. Results of ambient gamma-ray dose rate, atmospheric radioactivity and meteorological observation. JAEA-Data/Code 2013-006. Japan Atomic Energy Agency, 2013.

JAEA. Database for radioactive substance monitoring data. Japan Atomic Energy Agency. [Internet] Available from (https://emdb.jaea.go.jp/emdb/en/) on 17 February 2020.

Katata, G., M. Chino, T. Kobayashi et al. Detailed source term estimation of the atmospheric release for the Fukushima Daiichi Nuclear Power Station accident by coupling simulations of an atmospheric dispersion model with an improved deposition scheme and oceanic dispersion model. Atmos Chem Phys 15(2): 1029-1070 (2015).

KEK. Method to separate plume- and accumulated surrounding-contributions to peak count rate using pulse height distribution time histories at monitoring post. KEK Internal 2014-7. High Energy Accelerator Research Organization (KEK), 2015.

Moriizumi, J., A. Oku, N. Yaguchi et al. Spatial distributions of atmospheric concentrations of radionuclides on 15 March 2011 discharged by the Fukushima Dai-ichi Nuclear Power Plant accident estimated from NaI(Tl) pulse height distributions measured in Ibaraki Prefecture. J Nucl Sci Technol 57(5): 495-513 (2019).

Nishihara, K., H. Iwamoto and K. Suyama. Estimation of fuel compositions in Fukushima-Daiichi Nuclear Power Plant. JAEA-Data/Code 2012-018. Japan Atomic Energy Agency, Tokaimura, 2012.

Ohba, T., A. Hasegawa, Y. Kohayagawa et al. Body surface contamination levels of residents under different evacuation scenarios after the Fukushima Daiichi Nuclear Power Plant accident. Health Phys 113(3): 175-182 (2017).

Oura, Y., M. Ebihara, H. Tsuruta et al. A database of hourly atmospheric concentrations of radiocesium (^{134}Cs and ^{137}Cs) in suspended particulate matter collected in March 2011 at 99 air pollution monitoring stations in eastern Japan. J Nucl Radiochem Sci 15(2): 1-12 (2015).

Saito, K. and Y. Onda. Outline of the national mapping projects implemented after the Fukushima accident. J Environ Radioact 139: 240-249 (2015).

Terada, H., G. Katata, M. Chino et al. Atmospheric discharge and dispersion of radionuclides during the Fukushima Dai-ichi Nuclear Power Plant accident. Part II: verification of the source term and analysis of regional-scale atmospheric dispersion. J Environ Radioact 112: 141-154 (2012).

Terada, H., H. Nagai, K. Tsuduki et al. Refinement of source term and atmospheric dispersion simulations of radionuclides during the Fukushima Daiichi Nuclear Power Station accident. J Environ Radioact 213: 106104 (2020).

Terasaka, Y., H. Yamazawa, J. Hirouchi et al. Air concentration estimation of radionuclides discharged from Fukushima Daiichi Nuclear Power Station using NaI(Tl) detector pulse height distribution measured in Ibaraki Prefecture. J Nucl Sci Technol 53(12): 1919-1932 (2016).

Tsuruta, H., Y. Oura, M. Ebihara et al. First retrieval of hourly atmospheric radionuclides just after the Fukushima accident by analyzing filter-tapes of operational air pollution monitoring stations. Sci Rep 4: 6717 (2014).

Tsuruta, H., Y. Oura, M. Ebihara et al. Time-series analysis of atmospheric radiocesium at two SPM monitoring sites near the Fukushima Daiichi Nuclear Power Plant just after the Fukushima accident on March 11, 2011. Geochem J 52(2): 103-121 (2018).

UNSCEAR. Sources, Effects and Risks of Ionizing Radiation. Volume I: Report to the General Assembly and Scientific Annex A. UNSCEAR 2013 Report. United Nations Scientific Committee on the Effects of Atomic Radiation. United Nations sales publication E.14.IX.1. United Nations, New York, 2014.